

## High-resolution determination of coral reef bottom cover from multispectral fluorescence laser line scan imagery

*Charles H. Mazel*

Physical Sciences Inc., 20 New England Business Center, Andover, Massachusetts 01810

*Michael P. Strand*

Coastal Systems Station, Dahlgren Division, Naval Surface Warfare Center, 6703 West Highway 98, Panama City, Florida 32407

*Michael P. Lesser*

Department of Zoology and Center for Marine Biology, University of New Hampshire, Durham, New Hampshire 03824

*Michael P. Crosby*

National Oceanic and Atmospheric Administration and U.S. Agency for International Development, Washington, D.C. 20523

*Bryan Coles*

Raytheon Electronic Systems, 50 Apple Hill Drive, Tewksbury, Massachusetts 01876

*Andrew J. Nevis*

Coastal Systems Station, Dahlgren Division, Naval Surface Warfare Center, 6703 West Highway 98, Panama City, Florida 32407

### *Abstract*

A prototype in-water laser line-scanning multispectral fluorescence imaging system was evaluated for its ability to provide data that could be used to determine the quantitative distribution and abundance of various functional groups on coral reefs. The system collected fluorescence imagery in three spectral bands with 1 cm<sup>2</sup> resolution at sites in Florida and the Bahamas. Fluorescence excitation was at 488 nm, and imagery was collected in emission bands centered at 520, 580, and 685 nm. Ground truth data on bottom cover was collected by divers using conventional line transect and photographic quadrat methods. A set of classification rules based on the relative signal levels in the three fluorescence channels was developed to assign the image pixels to functional groups. Once the image was classified, percent cover data for the groups were computed for the full image and for subsets of the image chosen to simulate line transect, grid survey, and photographic quadrat surveys. The statistics of percent cover of various bottom types derived from the fluorescence image compared favorably with those determined by diver survey techniques. The results demonstrate that fluorescence imaging has the long-term potential to provide coverage of large spatial areas of coral reefs at high resolution, with automated classification and quantification of functional groups in the image.

---

### *Acknowledgments*

This work was supported by grants to C.H.M., M.P.L., M.P.S., and B.C. from the Coastal Benthic Optical Properties program of the Environmental Optics Program, Office of Naval Research, and to M.P.C. from the U.S. Man and the Biosphere Program. We thank the Caribbean Marine Research Center at Lee Stocking Island, Bahamas, Florida Keys National Marine Sanctuary (FKNMS), National Oceanic and Atmospheric Administration (NOAA), Harbor Branch Oceanographic Institution, and the crews of the R/V *Edwin Link*, NOAA ship *Ferrel*, the FKNMS R/V *Cool Hand*, and the Florida Institute of Oceanography R/V *Suncoaster* for field support. The authors thank C. Daniels (NOAA), J. Wheaton (Florida Marine Research Institute), R. Brock (NOAA), K. Potts (Environmental Protection Agency), and S. Baumgartner (NOAA) for their support and contributions in conducting the Crosby's Hump field work.

Increasingly, ecologists are asked to conduct surveys to obtain quantitative data in a nondestructive manner on the abundance and distribution of organisms. In benthic marine systems, this is particularly daunting because we are generally limited by the amount of time we can spend underwater to collect high-quality data. Specifically, our understanding of coral reef ecology is severely hampered by our inability to map and monitor large expanses of reef area over any reasonable temporal scale. Many techniques have been applied to the assessment of benthic community structure, including quantitative photography using still (Bohnsack 1979) and video (Whorff and Griffing 1992) systems. Additionally, comparisons of visual surveys, random-point quadrats, and digital images from still and video photogra-

phy have produced a variety of opinions on the best way to assess benthic community structure by considering the competing interests of data collection effort, analytical effort, and cost (Meese and Tomich 1992; Dethier et al. 1993; Leonard and Clark 1993).

The need for improved methods for assessing the areal coverage of different functional endmembers of coral reefs on large spatial and temporal scales has motivated the investigation of optical approaches, including aerial photography (Sheppard et al. 1995) and satellite and airborne multi- and hyperspectral remote sensing (Luzkovich et al. 1993; Mumby et al. 1998; Holden and LeDrew 1999). Any optical approach to monitoring coral reefs must include a mechanistic approach to the underlying reasons for changes in the optical signal(s) of choice. An emerging optical signal that has potential utility in this area is fluorescence of the benthic community. Hardy et al. (1992) investigated the application of laser fluorescence to the detection of coral bleaching by measuring reduction in the chlorophyll fluorescence signal. Simon-Blecher et al. (1996) used fluorescence spectral imaging to investigate the microdistribution of chlorophyll in corals.

Recent work investigating fluorescence properties of the coral reef environment for remote sensing and underwater imaging has led to the collection of large-scale laser-stimulated multispectral fluorescence imagery of coral reefs. Here we demonstrate the feasibility of performing automated classification of corals and other functional groups in the fluorescence imagery. Once assigned to categories of interest, the high-resolution data can be analyzed in a number of useful ways, such as by calculating percent cover. A fluorescence imaging technique could ultimately supplement or replace the time-consuming and cumbersome process of diver inspection at close range, thus expediting the process of mapping, and ideally assessing, the condition of reefs worldwide. This in turn would significantly enhance local, regional, and global efforts to better manage the plethora of natural and anthropogenic threats to coral reef biodiversity (Maragos et al. 1996).

#### Sources of fluorescence in the coral reef environment

*Corals*—All corals that host single-celled photosynthetic dinoflagellate endosymbionts (=zooxanthellae) will exhibit the characteristic deep red fluorescence (emission maximum at ~685 nm) from chlorophyll *a* (Chl *a*). The fluorescence emission is a by-product of the photosynthetic process, and the broad spectrum of wavelengths that can be utilized for photosynthesis will also result in chlorophyll fluorescence. In addition, many symbiotic corals contain host pigments that can exhibit fluorescence over a wide range of visible wavelengths (Catala 1959; Logan et al. 1990; Mazel 1995). Some of these host pigments have been identified (Matz et al. 1999) as variants of the green fluorescent protein (GFP) originally identified in hydroids by Morin and Hastings (1971) and isolated and described from the hydromedusae of *Aequorea victoria* (Prasher et al. 1992) and many scleractinian corals from the Indo-Pacific (Dove et al. 2001) and Caribbean (Labas et al. 2002; Mazel et al. 2003).

The various coral fluorescent pigments have differing excitation spectra (Mazel 1997; Matz et al. 1999), posing a challenge for selecting a single excitation wavelength or even an optimal range of wavelengths that will stimulate the fluorescence of all of them. Some of these pigments can be excited by long-wave ultraviolet radiation, but others will not respond to ultraviolet and are optimally excited at blue, green, or even orange wavelengths.

Not all zooxanthellate corals contain host fluorescent pigments, and among those that do, a great deal of variety has been observed in the emission spectra and fluorescence efficiency both between and within species and from one location to another. Intense host pigment fluorescence has recently been observed in several azooxanthellate specimens in the Indo-Pacific (personal observation). Knowledge of the factors controlling the expression of the fluorescence of host pigments is quite limited (Mazel et al. 2003).

The fluorescent bands observed in some coral skeletons (Boto and Isdale 1985) are not typically detected in measurements of healthy corals. This fluorescence may be measurable in dead corals or coral rubble that is not overgrown with a masking layer of algae. The source of this fluorescence is discussed in the Sediments section below.

*Other invertebrates*—Fluorescence of host pigments and of chlorophyll in symbionts has been documented in sessile cnidarians other than scleractinian corals, including various anemones, corallimorpharians, and zoanths. Gorgonians in the Caribbean have so far only been observed to contain chlorophyll, but with a particularly strong fluorescence signal. Fluorescence has also been observed in some hydroids and sponges and in mobile invertebrates such as shrimp, crinoids, polychaete worms (*Hermodice carunculata*), and nudibranchs. In most of these cases, there have not been quantitative measurements of the fluorescence spectral characteristics.

*Vertebrates*—There has been no systematic investigation of fluorescence in reef vertebrates. In situ observations indicate that there is fluorescence in some invertebrate chordates such as tunicates. Fish tend not to be fluorescent, but occasional instances of fluorescence have been observed. In some cases the fluorescence appears to arise from the fish itself, while in others it is associated with algae colonizing the surface of the animal (Ballantine et al. 2001).

*Macroalgae*—Reef macroalgae all contain chlorophyll, which exhibits a characteristic deep red fluorescence. The macroalgae fall into three groups—green (Chlorophyta), brown (Phaeophyceae), and red (Rhodophyta)—that differ in their characteristic photosynthetic accessory pigments. The green algae contain Chl *a* and *b*, whereas the brown algae contain Chl *a* and *c*. The red algae are distinctive in containing a phycobiliprotein complex that efficiently captures green light and transfers the energy to chlorophyll. The differences in accessory pigments result in systematic differences in excitation spectra for chlorophyll fluorescence (Topinka et al. 1990). The green and brown algae exhibit only chlorophyll fluorescence, but the red algae also have

emission peaks associated with phycoerythrin and phycocyanin, at  $\sim 580$  and  $660$  nm, respectively.

*Cyanobacteria*—Cyanobacteria contain chlorophyll and phycobiliproteins, as described for the Rhodophyta. Cyanobacteria are plentiful in the reef environment and can be found in symbiosis with sponges and ascidians (Wilkinson and Fay 1979; Larkum et al. 1987) and growing epiphytically on coral skeletons. They can also comprise part of the benthic microalgal community. Some forms of cyanobacteria are also coral pathogens (Rützler et al. 1983).

*Benthic microalgae*—The benthic microalgal community largely comprises a combination of diatoms, dinoflagellates, cyanobacteria, and chlorophytes, with the particular composition and quantity at any place and time a function of a range of factors. All contain Chl *a* and, as with the macroalgae, differ in the composition of their accessory pigments.

*Sediments*—Carbonate sediments are largely derived from calcareous algae and scleractinian corals (Tucker and Wright 1990). Organic components may be incorporated in the carbonate matrix during its formation. Some of this organic matter (humic and fulvic acids) is fluorescent and imparts a fluorescence signature to the carbonate, as has been documented for banding patterns in the skeletons of reef corals (Boto and Isdale 1985; Matthews et al. 1996). Fluorescence excitation and emission spectra of other sources of carbonate sediment material, including a variety of calcareous algae, gastropods, echinoids, bivalves, and calcareous worm tubes, are very similar to those of corals (Allison unpubl. data). Our direct measurements of sediment fluorescence spectra (unpubl. data) confirm their similarity to those of the carbonate sources in the reef environment. The excitation/emission matrix reveals broad excitation and emission bands characteristic of materials containing a variety of fluorescing substances. The primary excitation and emission maxima fall at  $\sim 370$  and  $\sim 470$  nm, respectively, but the breadth of the spectra indicates that there can be fluorescence stimulation and emission over a wide range of wavelengths.

*General comments on fluorescence*—The intensity of the emission from any source of fluorescence will be a function of many factors. These include, but are not limited to (1) the quantum yield, defined as the ratio of photons fluoresced to photons absorbed, which can vary even within a healthy population; (2) the overlap between the spectral distribution of the excitation source and the excitation spectrum of the molecule; (3) fluorescence quenching effects due to the chemistry of the microenvironment or reabsorption of emitted radiation (packaging effects); and (4) nonradiative energy transfer to another molecule (as in the energy transport chain from the phycobiliproteins to chlorophyll). From the point of view of a sensor such as the laser imager described here, other effects can come into play, such as (1) the quantity of the fluorescing material per unit area of a specimen surface, (2) the uniformity of the illumination from one sample point to another, and (3) optical attenuation in the water column. The net result is that the observed intensity of fluorescence can be quite variable for a given method of illu-

mination and detection, even for a particular fluorescing substance within any of the functional groups discussed above.

## Methods

*Field sites*—Fluorescence images of reef sites were made as part of the Coastal Benthic Optical Properties research program at locations in the Dry Tortugas, Florida, in August 1996 and around Lee Stocking Island (LSI), Bahamas, in May 1998. The Dry Tortugas site, designated Crosby's Hump, is a low-relief coral patch reef community located on a topographic high at  $24^{\circ}32.63'N$ ,  $082^{\circ}56.9'W$ ,  $\sim 8$  nautical mi. south of the lighthouse at Loggerhead Key. The depth to the bottom was 18 to 20 m, and height of features above the bottom was typically  $<0.5$  m. At LSI, imagery was collected at North Perry Reef, a spur and groove formation on the windward side of the island at  $\sim 23^{\circ}46.98'N$ ,  $076^{\circ}06.05'W$ . The depth to the sand was  $\sim 17$  m. The coral head that was the focus of the work had a relief of 2 to 3 m above the seafloor.

*Laser fluorescence imaging*—Fluorescence of the seafloor was imaged with a prototype Fluorescence Imaging Laser Line Scanner (FILLS, Raytheon Electronic Systems Corp.) operated by the Coastal Systems Station. FILLS sweeps a 488-nm (blue) laser beam over the bottom in a scan perpendicular to the sensor's direction of motion (Strand et al. 1997). The rotating output optical assembly and the four rotating input optical assemblies are mounted on a common drive shaft to ensure mechanical synchronization of the laser and receiver spots on the seafloor. Each receiver consists of a rotating input optical assembly, a controllable aperture assembly, a photomultiplier tube (PMT), a preamplifier and signal conditioning electronics, and an analog-to-digital converter. The four detector channels record the reflected blue light through a 488-nm interference filter—10 nm full width at half maximum (FWHM)—and fluorescence emission through interference filters centered at 520 nm (green, 10 nm FWHM), 580 nm (orange, 10 nm FWHM), and 685 nm (red, 20 nm FWHM). The green channel records coral and carbonate sediment fluorescence, the orange channel records the fluorescence from phycoerythrin and some corals, and the red channel records chlorophyll emission. The FILLS system was operated at night, thus avoiding interference from reflected solar illumination and solar-induced fluorescence.

The input/output optical assemblies employ four-faceted mirrors, yielding four  $90^{\circ}$  scan lines per rotation of the drive shaft. Scan line (cross track) imagery is formed from the center  $70^{\circ}$  portion of each scan line by digitizing the electrical output from each receiver to 12 bits at a user-selectable number (512, 1,024, 2,048, or 4,096) of pixels per scan line. This results in a swath width  $\sim 1.4$  times the sensor altitude above the bottom. Two-dimensional imagery is formed by platform motion, ensuring that successive scan lines are displaced from each other. The pixel size depends on sensor altitude, tow speed, scan rate, and the number of pixels per scan line. For the surveys described here, the operating altitude was  $\sim 7$  m, yielding a nominal 10-m swath width digitized to 1,024 pixels. Vignetting effects on two of the chan-

nels limited the usable swath width to  $\sim 8$  m (824 pixels). Each pixel corresponded to  $\sim 1$  cm<sup>2</sup> on the bottom.

FILLS, like other laser line scan sensors, reduces the detrimental effects of water column backscatter and blur/glow/forward scatter by producing imagery from a very small laser spot and small, synchronously scanned receiver spots. The resolution of the sensor is largely defined by the highly collimated laser beam, which has a nominal beam divergence of 1 mrad in the typically clear waters where coral reefs are found. The receiver spots on the seafloor are roughly rectangular. The cross-track widths of the receiver spots are typically 10 mrad or less. The user controllable depth of field of the sensor determines the along-track length of the receiver spot. The depth of field is controlled by the upper imaging range (UIR) and lower imaging range (LIR) of the sensor, which are set to bracket the sensor altitude. Physically, the UIR and LIR of each receiver are controlled by an aperture assembly in front of the PMT. For FILLS, the minimum UIR is  $\sim 4.6$  m (15 ft.). Practical maximum upper and lower imaging ranges are set by water clarity conditions.

Monochromatic laser line scan sensors have been demonstrated to produce good image quality at ranges up to five to six beam attenuation lengths (Strand 1997), where a beam attenuation length is defined as the distance over which the beam intensity is reduced by a factor of  $1/e$ , or  $\sim 63\%$ , by absorption and scattering. The beam attenuation length for any wavelength will be a function of the inherent optical properties of the water column. In the surveys described here, the range was  $< 1.5$  beam attenuation lengths for the elastic, green, and orange receiver channels and  $< 4.5$  beam attenuation lengths for the red receiver channel. Furthermore, the range was  $< 1.5$  beam attenuation lengths for the blue laser. Spatial spreading of a laser beam is negligible at 1.5 beam attenuation lengths. The evident high image quality of the FILLS images presented here is understandable because the resolution of laser line scan sensors is largely determined by the laser spot size.

The prototype FILLS sensor package is 2.3 m long and 0.55 m in diameter and weighs  $\sim 480$  kg in air. The power consumption is  $\sim 7.5$  kW. The sensor can be housed in a streamlined body that is towed behind a survey vessel, but for the Crosby's Hump and North Perry Reef projects, FILLS was attached beneath the research submersible *Clelia* operated by the Harbor Branch Oceanographic Institution. During a mission, the FILLS operator riding in the submersible viewed enhanced imagery on the real-time display console, enabling adjustment of system settings and allowing for selected data to be stored in raw format on the console's storage disk. On return to the ship, the raw data were transferred from the console storage disks to the ship's lab for quick turnaround data processing. Waterproof photographic-quality prints of enhanced FILLS data were generated in the field, permitting divers to take the prints to the data collection site for identification of features in the FILLS imagery.

At both field sites, the submersible carrying the FILLS sensor was manually steered by the submersible operator along a transect line that had been laid on the bottom by divers. The transect line was marked at 1-m intervals with fluorescent flagging tape. The imagery for Crosby's Hump comprised a swath 824 pixels wide by 4,096 pixels long

(3,375,104 pixels). The FILLS imagery at Crosby's Hump was collected  $\sim 2$  months after the diver survey of the site, over the center line of the three transect lines (*see Diver Surveys*, below). At the North Perry Reef site, data were collected over a transect line 150 m in length. Analysis of the FILLS imagery for this site focused on one coral head comprising a  $676 \times 662$ -pixel subset (447,512 pixels) of the data set.

*Laser image data processing*—FILLS raw data were collected at carefully controlled gain to prevent saturation of brightly fluorescing corals. The raw data were preprocessed (Nevis 1999) before analysis and display to compensate for three effects. First, slight variations between the rotating mirror facets in the FILLS scanning mechanism were magnified in the data, resulting in visual striping of the data in the cross-track direction. The striping was corrected by computing the mean discrete Fourier transform (DFT) of the image columns (perpendicular to the striping), isolating and suppressing the frequencies associated with the striping and then applying the inverse DFT. Second, the high dynamic range of the received signals presented a challenge for display. A linear mapping of the signals to the display intensity made it difficult to display features associated with low signal levels without saturating the display in the regions of high signal level. Applying a  $\log_{10}$  transformation and re-scaling the image to the full 12-bit dynamic range allowed features in regions of both high and low signal level to be successfully displayed. Third, there were signal level variations associated with the varying range to different parts of the scene. These variations were due to topographic changes, slant range effects, and variations in the submersible's altitude and orientation. The varying range resulted in varying effective attenuation of the signals across the scene. A phenomenological procedure was developed to partially compensate for the slant range and altitude variations. To help equalize the regions of uneven background signal level, the image background was estimated and corrected by using overlapping least squared error line segments. The final preprocessing step was to manually apply a histogram clip on each fluorescence channel to maximize contrast of the image background without significant saturation of the brightly fluorescing features in the display. For ease in visualization, the three fluorescence channel images were combined in a pseudocolor RGB image, with the red fluorescence channel assigned to the red display channel, the green to the green, and the orange to the blue.

After image preprocessing, a set of image classification rules was developed using the ENVI software package (Research Systems Inc.). The rules were developed by examining the data values of the three fluorescence bands for various features in the image, writing routines that separated the data on the basis of these pixel values, and iteratively refining these routines based on observations of how well the classified image corresponded to the original image. Thus the classification scheme was based on the characteristics of the processed image and not on a first-principles approach grounded on the fluorescence spectral properties of the image features. The two approaches are related because the spectral distribution of fluorescence in a subject will de-

Table 1. Classification categories for the Crosby's Hump data, their appearance in the pseudocolor RGB display, and a description of the algorithm rules. The R, G, and B referred to in the third column are the red, green, and blue pixel values in the displayed image, which are derived from the red, green, and orange fluorescence data channels, respectively. The classification process was applied in the sequence (top to bottom) shown in the table. Once a pixel had been assigned to a category, it was removed from further consideration.

Category	Appearance in RGB image	Basis for classification
Shadows and nonfluorescent targets	Black	R, G, and B below a threshold
Corals, anemones, zoanthids, corallimorphs	Generally bright, may be white, yellow, orange, turquoise, or red depending on mix of chlorophyll and host pigments	R, G, and B or R and G above designated thresholds
Sand, rubble, bare substrate	Green, dominated by carbonate fluorescence	$G > R$ and $G > B$
Red algae, cyanobacteria	Light blue-purple, resulting from a mix of chlorophyll and phycoerythrin	$B > R$ and $B > G$ , and R, G, and B above designated thresholds
Sponge <i>Xestospongia muta</i>	Distinctive dark blue-purple, probably arising from phycoerythrin fluorescence of symbionts	$B > R$ and $B > G$
Gorgonians, macroalgae	Red from chlorophyll-only emission; gorgonians generally brighter, but difficult to distinguish because of signal variations due to yield, imaging range, etc.	$R > G$ and $R > B$ , and all channels above or below designated thresholds
Unknown	Various	All pixels that did not fall into any of the above categories

termine the relative response in each of the three fluorescence detection channels, but the radiometric relationships are not necessarily conserved. A subject with only chlorophyll fluorescence will contribute only to the red fluorescence channel, whereas a subject with chlorophyll plus phycoerythrin will register in the orange and red channels, but not the green. In the latter case, the mapping of the red fluorescence channel to the red display channel and of the orange fluorescence channel to the blue display channel will result in a pixel that is a combination of blue and red. This will appear as some color ranging from blue to purple to red, depending on the relative levels of the two signals. A coral exhibiting the green fluorescence of the host pigments plus the red fluorescence of the chlorophyll in the zooxanthellae would map to the green and red channels, producing a yellow to orange pixel in the display.

For the Crosby's Hump data set, the classifier rules were developed using one-half of the full image and then applied to the other half with no further changes. The seven categories for classification were chosen based on visual inspection of the image and a subjective judgment as to the features that could be distinguished. The correlation between image features and actual specimens on the bottom was verified for numerous specimens by diver observation. The classification categories were (1) bright white, yellow, orange, or turquoise targets (cnidarians, consisting of scleractinian corals, anemones, zoanthids, and corallimorpharians); (2) sand, rubble, and bare substrate; (3) red algal turf (red algae and cyanobacteria); (4) black (nonfluorescent targets and shadowed pixels); (5) red and bright-red targets (gorgonians, some scleractinian corals, and macroalgae); (6) barrel sponge *Xestospongia muta*; and (7) unknown. The classification process is outlined in Table 1. The threshold values used for making decisions were selected by trial and error as part of the iterative process described above. Quantitative values for the thresholds used are not presented because they have no significance independent of this particular image. The output of

the process was a new image with each pixel assigned a color corresponding to its classification. Three targets that appeared red-fluorescent only were recognizable from the image as scleractinian corals. This judgment was confirmed by in situ observation. The pixels associated with these targets were reassigned to the "bright" (cnidarian) category.

A similar procedure was applied to the data from North Perry Reef. The rules used for the North Perry Reef image were similar but not identical to those used for the Crosby's Hump image because the FILLS system had been reconfigured between surveys and the resulting images were not equivalent mappings of the raw data. The image data were analyzed only for one large coral head that was extensively investigated by divers.

The categorized images were then analyzed for percent cover in several ways with the MATLAB software package (Mathworks Inc.). These analyses were selected either for direct comparison with the results of the diver ground truth surveys or to explore the kinds of statistical studies that this new data set makes possible. For the Crosby's Hump data, the total number of pixels that fell into each class was tabulated and the percent cover of each type was computed. Continuous line transects were simulated by computing the coverage statistics for each of the 824 strips, 1 pixel wide, extending the full 4,096-pixel length of the image. This was done to explore the sensitivity of the computed statistics to the choice of transect line location. The 4,096 pixels in each such simulated transect corresponded to 0.12% of the full data set.

Grid-based sampling schemes are an alternative approach to habitat mapping, and a simulated grid sampling was performed on the Crosby's Hump data by computing the total statistics for 320 squares of  $11 \times 11$  pixels centered at a nominal 1-m (100-pixel) spacing in the image ( $8 \times 40$ -m grid). This amounted to a total of 38,720 pixels, or just  $>1\%$  of the total pixels in the image.

The sizes of all of the objects classified as cnidarian in

the Crosby's Hump image were computed by counting the number of pixels associated with each such object. Objects were defined as sets of connected pixels, where pixels were considered connected if they touched horizontally, vertically, or diagonally. The size-frequency distribution (Bak and Meesters 1998) of the objects was then determined.

For the North Perry Reef image, the only analysis performed was a simulated 0.25-m<sup>2</sup> photographic quadrat sampling, analogous to the diver ground truth survey conducted at this site (*see Diver Surveys*, below). The analysis was restricted to the bright target category because the relief at this site resulted in a variation in signal levels that made the more detailed classification unreliable. A random number generator was used to position a square 50 × 50 pixels on the image, and the percentage of pixels in that square that were classified as "bright" was computed. Squares that did not fall entirely on the coral head were excluded from analysis. Statistics were computed for five sets of 50 simulated quadrats each.

*Diver surveys*—Identification of specific features in the FILLS imagery was conducted at both field sites by divers carrying copies of the images printed on waterproof paper. Species, genus, or functional group identification was made visually.

The benthic habitat at Crosby's Hump was characterized by divers employing a line-point intercept method (Loya 1978; Ohlhorst et al. 1988; Crosby and Reese 1996) along the 50-m FILLS transect line and additional parallel 50-m transect lines ~30 m to the east and west of that line. The benthic habitat type was recorded at 1-m intervals along each of the three transect lines. In addition, a comprehensive census for diversity of stony coral and gorgonian species was conducted by a diver search of the ~3,000-m<sup>2</sup> area encompassed by the three transect lines for a total period of 60 min.

At North Perry Reef, 34 randomly placed 0.25-m<sup>2</sup> photographic (35 mm) quadrats were sampled using a Nikonos V with a 15-mm lens and synchronized strobes using a quadropod with scale (2 cm) as described in Witman (1985). Individual photographs were digitized into TIFF images and the projected surface area of the dominant functional groups was analyzed using NIH Image software. For each photograph, the entire quadrat was analyzed for hard corals, soft corals, sponges, macroalgae, and bare consolidated carbonate substrate.

## Results

Figure 1A–E shows the reflectance channel image, the three fluorescence channel images, and the corresponding pseudocolor image from an 824 × 824 pixel section of the survey swath at Crosby's Hump. It is immediately striking that virtually everything in the image is fluorescing to some degree, with many features standing out in strong contrast. The bright targets correspond to scleractinian corals, anemones, and zoanthids, but not all similar specimens appear as bright targets. The large red target just below the center of Fig. 1E was identified by in situ observation as a specimen of *Montastraea faveolata*. The chlorophyll in the zooxan-



Fig. 1. Grayscale images of the Crosby's Hump site produced by the (A) reflectance (488 nm); (B) green (520 nm) fluorescence; (C) orange (580 nm) fluorescence; and (D) red (685 nm) fluorescence FILLS channels, and (E) a composite pseudocolor RGB presentation of the fluorescence channel data. To make the RGB image, the red fluorescence channel was mapped to the red display channel, the green fluorescence channel to green, and the orange fluorescence channel to blue. The images are each 824 × 824 pixels.

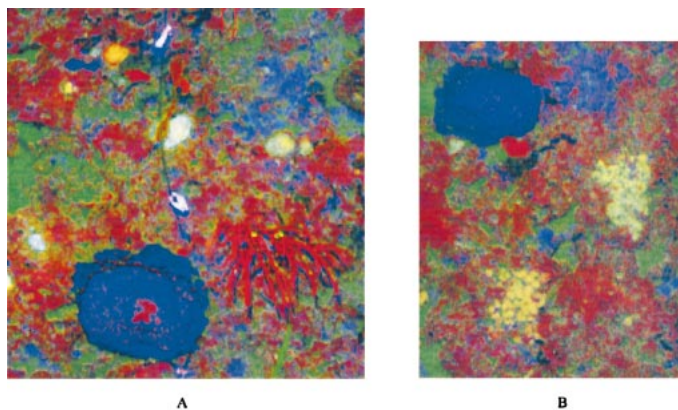


Fig. 2. Details of portions of the FILLS images from Crosby's Hump. (A) A barrel sponge (*Xestospongia muta*) is evident at the bottom of the image. Algae is growing in the center of the sponge, indicated by the red fluorescence. To the right of the sponge is the gorgonian *Pseudoplexaura* sp. Several hard corals are evident as bright targets. (B) The mottled orange and yellow-green patches are colonies of the zoanthid *Palythoa caribaeorum*. This physical appearance was characteristic of this species in the images.

thellae contributed the red fluorescence, but this particular specimen lacked host pigments stimulated by 488-nm excitation. Other *M. faveolata* specimens in the image fluoresced intensely in the green and orange bands.

Many features can be readily recognized in the laser imagery. A detail of a different portion of the image (Fig. 2A) clearly shows a red-fluorescing gorgonian (*Pseudoplexaura* sp.) to the right of a barrel sponge (*X. muta*). Algae growing in the center of the sponge are distinguished by their red chlorophyll fluorescence. Two of the fluorescent marker tags on the transect line appear as bright targets, and numerous corals appear as roughly round, brightly glowing targets.

Observation by divers identified the mottled orange and yellow-green patches in Fig. 2B as colonies of the zoanthid *Palythoa caribaeorum*. These appear in numerous places in the full image with a variety of fluorescence signatures. The combination of moderately bright fluorescence and this characteristic physical appearance makes them easy to identify and suggests that a combination of spectral and shape classification rules could prove very powerful in interpreting the laser fluorescence imagery.

A careful examination of the imagery, supported by diver ground truth investigation, revealed that the pixels classified as black were largely associated with three sources: shadows resulting from the viewing geometry, fish, and the sponge *Callyspongia vaginalis*.

Figure 3 shows the same section of the FILLS image as in Fig. 1A–E, with each pixel assigned a color according to the output of the classification rules. Note that the red fluorescent *M. faveolata* specimen discussed above appears in the bright category in this image. This and two other specimens were manually transferred from the bright red category, as described in Methods.

The results of the computations of percent cover of the bottom types in the FILLS imagery for Crosby's Hump are summarized in Table 2. The results for the full image and the subsampling of pixels at the grid intersections are quite

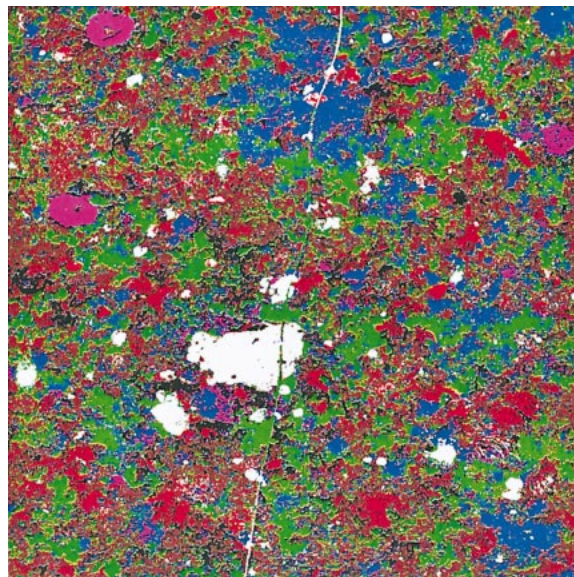


Fig. 3. Results of classification of the FILLS image of Fig. 1 into six bottom type categories: white = corals, anemones, zoanthids; red and brown = gorgonians; green = sand or bare substrate; blue = red algal turf; black = shadows, fish, and the sponge *Callyspongia vaginalis*; purple = the barrel sponge *Xestospongia muta*; pink = unknown. The "unknown" pixels are widely scattered in the image and may not be evident in this reduced presentation.

similar, indicating that this subsample, comprising ~1% of the total number of pixels, provides a good approximation to the full data set.

Table 3 summarizes the percent cover of the benthic habitat types determined from the diver survey at Crosby's Hump. A total of 10 species of stony coral, 1 species of Millepora, and 16 species of gorgonians were identified in the 3,000-m<sup>2</sup> area encompassed by the three transect lines. *Montastraea cavernosa* and *Siderastrea siderea* were the most frequently occurring stony coral. *Eunicea* sp. and *Pseudopterogorgia americana* were the two most frequently occurring gorgonians. Barrel sponges, *X. muta*, were frequently observed in the study site.

Table 2. Percent bottom type cover at Crosby's Hump derived from the FILLS imagery for all pixels in the image, and for groups of 11 × 11 pixels at a 1-m grid spacing. Standard deviations are computed from the coverage results computed for the simulated transect lines (Fig. 4).

Benthic type	Mean (all pixels)	Mean (pixels at grid inter- sections)	SD (from simulated transect lines)
Bare substrate (sand, rubble)	26.1	27.6	3.0
Red algae, cyanobacteria	12.5	11.5	3.4
Gorgonian	45.7	45.2	4.9
Cnidarian	2.5	2.9	1.2
Sponge	3.0	3.5	1.0
Black (shadows, fish, <i>Callyspongia</i> )	8.4	7.6	1.7
Not classified	1.8	1.7	0.3

Table 3. Summary statistics of percent cover of benthic habitat type for three 50-m line-point intercept transects at Crosby's Hump, June 1996. SE, standard error; Min., minimum value; Max., maximum value.

Benthic type	Mean	SE	Min.	Max.
Pavement	0.0	0.0	0.0	0.0
Rock/rubble	19.4	4.1	12.0	26.1
Sand	5.4	1.3	4.0	8.0
Dead coral	0.0	0.0	0.0	0.0
Macroalgae	1.3	1.3	0.0	4.0
Gorgonian	57.5	2.4	54.0	62.0
Zooanthid	0.0	0.0	0.0	0.0
Coral	11.0	5.2	2.0	20.0
Sponge	5.4	1.7	2.2	8.0

Figure 4A–G shows the variation in percent cover for each FILLS bottom type for the simulated one-pixel wide continuous line transects. The average values for all pixels in the image are indicated on the graphs, as are the averages for the simulated grid square sampling and the boundaries for plus or minus one standard deviation of the simulated line transect data.

In Fig. 5A, only the pixels classified as cnidarian are shown. Assuming the classification is largely correct, this form of category-specific image provides insight into the size and spatial distributions of this functional endmember. The size-frequency distribution for the cnidarian targets in the full image is summarized in Table 4, in which the size classes are related logarithmically. The distribution is heavily skewed toward small objects.

At the North Perry Reef site, the FILLS image analysis and ground truth investigations were focused on one coral head. Figure 6 shows the pseudocolor fluorescence image for that site. There is a clear falloff in intensity, especially of the red channel, toward the bottom and left of the coral head because of the change in distance of the reef surface from the sensor. The coral head is somewhat rounded, and the top, near the center of the image, is  $\sim 2.5$  m above the surrounding sand. The portion of the head at the bottom of the image is  $< 1$  m above the sand. The attenuation of the deep red chlorophyll emission is significant enough to require correction for image equalization, but the detailed relief information required to make such a correction was not available. Note that the variation in appearance of the sand surrounding the reef is almost certainly associated with the presence of patches of benthic microalgae.

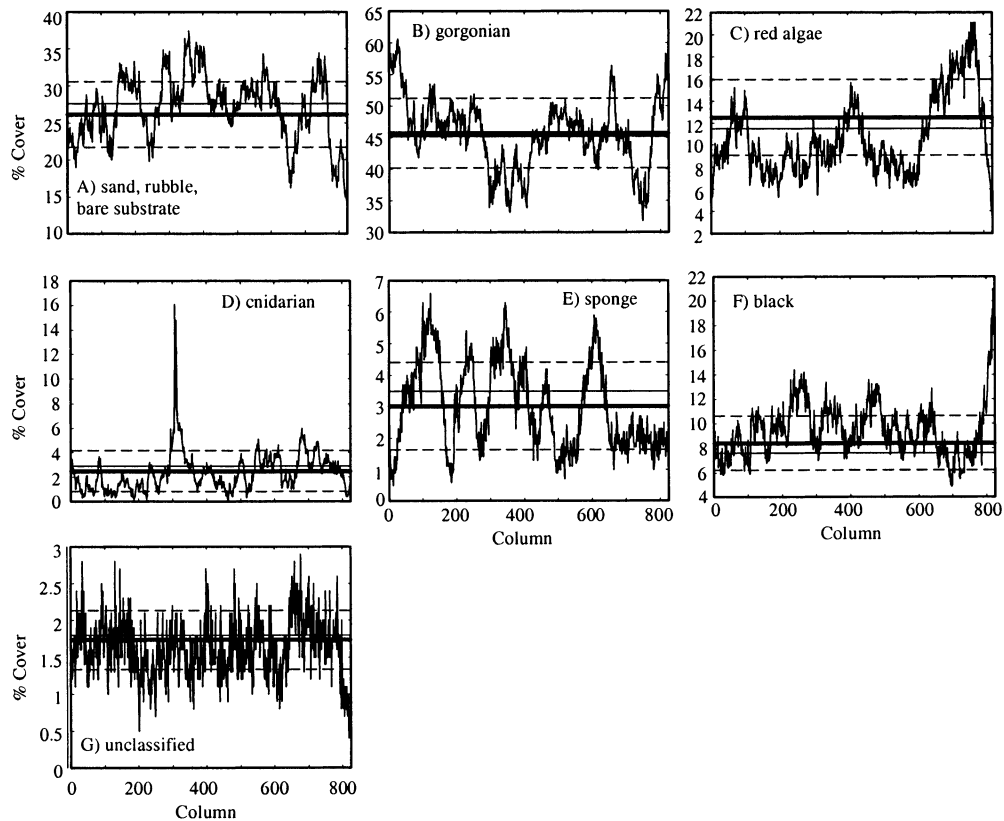


Fig. 4. Plots showing the percent cover statistics for columns of data one pixel wide, extending the full 4,096-pixel length of the FILLS image for Crosby's Hump. The global average for all pixels is indicated by the thick horizontal line, the interval for plus or minus one standard deviation by the dashed horizontal lines, and the average of all pixels in squares  $11 \times 11$  pixels centered at 1-m grid intervals by the thin horizontal line. (A) Sand, rubble, bare substrate; (B) gorgonians; (C) red algae and cyanobacteria; (D) bright targets (cnidarians); (E) barrel sponges; (F) black pixels (shadows, fish, some sponges); (G) not classified.



Fig. 5. Image showing only the pixels classified as "bright" in Fig. 3. These pixels largely correspond to scleractinian corals, anemones, and zoanthids.

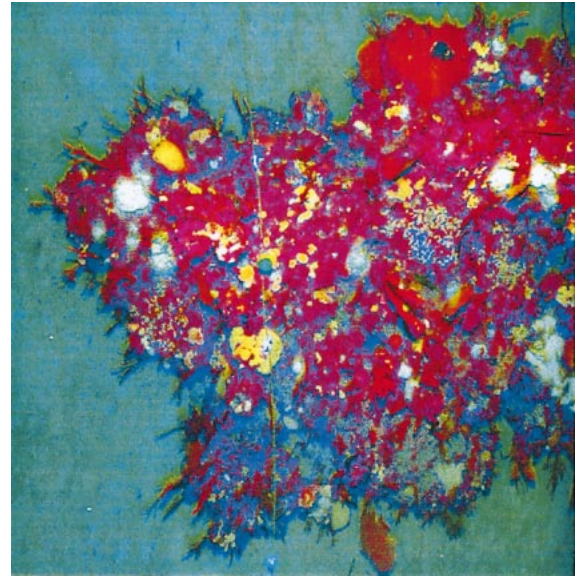


Fig. 6. Pseudocolor fluorescence image of a coral head at the North Perry reef site.

The distinctive variation in appearance of objects in Fig. 6 suggests that the same type of feature classification and statistical analysis described for the Crosby's Hump site could be performed for this image, but the nonuniform variation in signal intensity made this operation unreliable. Analysis of the image data was restricted to determination of percent coral cover because the bright signals from corals are the most distinct features in the image, and the green and orange emissions most responsible for these are the least affected by the differences in path length. The clusters of small bright targets evident in Fig. 6, 7B are colonies of *Porites porites*, and are very recognizable in the imagery.

To restrict the analysis to the reef surface, it was necessary to remove the sand pixels from the data. Feature classification rules similar to those used for the Crosby's Hump data

were developed to isolate the sand (Fig. 7A) and coral (Fig. 7B) pixels in the image. The large bright red target at the top right of the image (Fig. 6) was confirmed by divers to be a specimen of the scleractinian coral *Colpophyllia natans*. As for similar features in the Crosby's Hump data, this feature was transferred from the red to the bright category. The full image is  $676 \times 662$  pixels, for a total of 447,512 pixels. Of these, 160,016, or 35.8%, were classified as sand. Of the remaining 287,496 pixels, 31,006, or 10.8%, were classified as "bright." The diver investigations of the site indicated that at this location the bright targets were almost exclusively scleractinian corals.

Analysis of the 34, 0.25-m<sup>2</sup> photographic quadrats from the diver survey indicated that the percent cover of scleractinian corals ranged from 1.6 to 83.3% per quadrat, with a mean of 23.2% and 17.8% SD. The results of the photo-

Table 4. Size-frequency distribution of bright targets (nominally cnidarians) in the fluorescence imagery from Crosby's Hump, determined by counting the pixels associated with each unique target. The size ranges correspond to equal intervals of the natural logarithm of the size (Bak and Meesters 1998). Each pixel corresponds to approximately 1 cm<sup>2</sup>.

Size interval (in pixels)	Number of occurrences
1	4,447
2-3	1,906
4-7	795
8-20	436
21-55	173
56-148	86
149-403	49
404-1,097	22
1,098-2,981	4
2,982-8,103	1
8,103-22,026	1

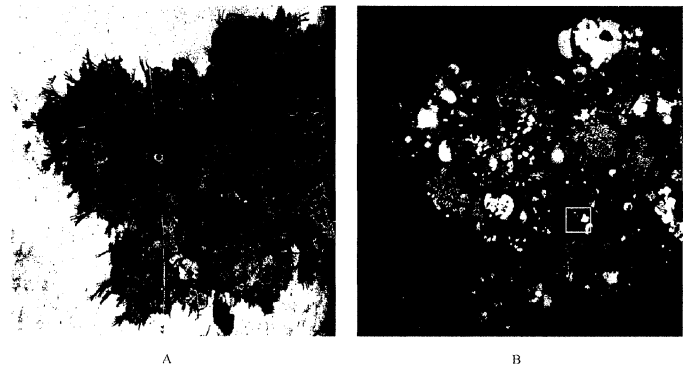


Fig. 7. Portions of the laser fluorescence imagery for North Perry Reef classified as sand and coral are indicated by the white pixels in (A) and (B), respectively. The white square in (B) indicates the size of a representative selection  $50 \times 50$  pixels ( $\sim 50 \times 50$  cm on the reef) used to compute 0.25-m<sup>2</sup> quadrat statistics for coral cover from the FILLS data.

Table 5. Coral percent cover statistics for 34 photographic quadrats from the diver survey and five runs of 50 simulated quadrats each from the FILLS image data analysis for the North Perry Reef site. SE, standard error; Min., minimum value; Max., maximum value.

	Mean	SE	Min.	Max.
Photo quadrats ( $N = 34$ )	23.2	17.8	1.6	83.3
FILLS data ( $N = 50$ )	14.4	13.7	0.04	64.8
FILLS data ( $N = 50$ )	11.3	12.8	0.12	66.2
FILLS data ( $N = 50$ )	11.5	12.1	0.44	61.0
FILLS data ( $N = 50$ )	10.5	14.0	0.04	84.0
FILLS data ( $N = 50$ )	11.3	13.1	0.04	65.1

graphic analysis and of five separate quadrat simulation runs on the classified FILLS data, with 50 simulated quadrats in each run, are summarized in Table 5.

## Discussion

The FILLS system produces high-resolution multispectral fluorescence images of reef surfaces with large spatial coverage compared to other in situ methods. Features in the pseudocolor three-channel laser fluorescence images of the reef sites examined here are clearly more distinct than in the black and white reflectance images or in the individual fluorescence channel images. We attempted here to use the data from this prototype fluorescence laser line scanner to implement an algorithm for reef endmember classification. A major benefit of such a system would be a more detailed characterization of larger spatial areas than can be achieved by current diver survey techniques. The FILLS sensor is not practical for general use in its present form because of its size and its power and logistics support requirements. However, the prototype unit has successfully executed several proof-of-concept surveys to investigate the potential benefits of the technology and of the analytical approach.

The initial work with the FILLS system indicates that we can say with a high degree of certainty that nearly all of the targets that fluoresce brightly in the green wavelength band are cnidarians, but that not all cnidarians fluoresce brightly in this band. It was impractical to locate on the seafloor the source of every bright pixel in the images, but in every case that isolated bright pixels were spot-checked, a cnidarian was found, as small as 0.5 cm diameter. Several large corals in the Crosby's Hump imagery exhibited only the characteristic red chlorophyll fluorescence originating in their symbiotic zooxanthellae. There are two possible explanations for this observation: (1) these corals did not contain fluorescent pigments in the host tissues or (2) these corals did contain host fluorescent pigments, but their fluorescence was not excited by the 488-nm wavelength of the FILLS laser. A common host pigment for Caribbean corals, designated "486" in Mazel (1997) for the location of its emission peak, is not stimulated effectively by 488 nm. Several of the corals that appeared red in the laser imagery were found by direct measurement to contain this pigment. The choice of laser wavelength for FILLS was constrained by available technology, and in future, it may be possible to incorporate a laser that

is more effective at stimulating all of the coral host pigments. Use of more than one laser might be desirable, both to capture the greatest variety of fluorescence responses and to enable more sophisticated classifications, such as distinguishing among the major algal groups based on differences in excitation spectra for the same emission (Topinka et al. 1990). As our understanding of the nature and extent of fluorescence in the reef environment increases, we will be in a better position to define the classification limits of the technology and to design improvements that will enhance its capabilities.

The FILLS imagery can be used to distinguish among functional groups with some degree of success. Its ability to make more specific identifications is limited. Anything that contains chlorophyll shares an emission at  $\sim 685$  nm. Although there are some seemingly systematic differences in the efficiency of that emission between groups, this has not been investigated enough to be exploited effectively. Fluorescent pigments are widespread in cnidarian host tissues, and measurements to date (Mazel 1995, 1997) indicate that pigments with the same spectral characteristics can be found in a wide variety of species. This makes it difficult to identify cnidarians to species or even genus level on the basis of their fluorescence signatures alone. The brightest round features tend to be colonies of *M. cavernosa*, but colonies of other species can appear just as bright. Some genera or species are recognizable by the combination of their color and shape in the imagery, as was the case for colonies of *P. caribaeorum* (Fig. 2B) and *P. porites* (Figs. 6, 7B). Of the sponges specifically noted in the FILLS and diver surveys, *C. vaginalis* was distinctive in being almost the only benthic organism manifesting no fluorescence signal whatsoever. The barrel sponge, *X. muta*, exhibited an orange fluorescence (mapped to blue in the pseudocolor imagery) probably associated with cyanobacterial symbionts, although this requires further investigation. *Xestospongia* is easily recognized in the imagery by its distinctive shape.

Taking into account the current limitations in making fine discriminations from the FILLS imagery, there is good correspondence between the results from the FILLS data analysis and from the diver surveys at the two research sites (Tables 2, 3, 5). For Crosby's Hump, we can compare the value of 26–28% bare substrate for FILLS to the value of 24.8% for the combined categories of pavement, rock/rubble, sand, and dead coral from the diver survey. The mean coral cover derived from the fluorescence image was  $<3\%$  for FILLS, compared to 11% for the diver survey data. The diver transect line results varied from a low of 2.0% on one of the lines to a high of 20.0% on another. As the simulated line transect statistics shown in Fig. 4D indicate, the percent cover can be quite variable from line to line and can depend strongly on the presence of just one or two large coral heads. The transect line followed by the divers and by the submersible pilot was fixed at both ends, but not at intermediate points, and moved somewhat under the influence of currents. The FILLS survey was conducted 2 months after the diver survey, so the exact line followed by FILLS was almost certainly not identical to that followed by the divers. There is also the question of how much subjective judgment comes into play in a diver visual survey with a limited number of

sample points. The diver makes the determination of what is under a discrete marked point on a transect line, and there could be a bias to register a point as “coral” if the coral specimen is offset by only a centimeter or two from the current position of the line. Because there were only 50 marked points on each diver survey line, any assignment of a point to a category counts for 2% in the totals. This makes the diver survey results highly sensitive to a small number of decisions made in the field.

Pixels classified as either “red” or “bright red” (resulting from emission from chlorophyll alone) in the Crosby’s Hump FILLS imagery were classified as gorgonians for this analysis. In other circumstances, this red fluorescence could arise from macroalgae, but at this site, the diver investigations revealed a preponderance of gorgonians and relatively low macroalgal cover. It is hoped that with further refinements of the FILLS hardware and associated image processing, the need for diver investigations as a means of quality control would be reduced.

At the North Perry site, we see (Table 5) that the standard deviations and data ranges for the analyses of the photographic quadrats and of the simulated quadrats are similar, whereas the mean cover calculated from the former is on the order of twice that of the latter. The reasons for the magnitude of this difference are not entirely certain, but some of it could be accounted for by the nature of the classification and area computation processes for the two methods. For the FILLS data, once the classification rules were established, the counting of image pixels was completely automated. The only discretion exercised was the manual transfer into the coral category of one large coral colony (verified by divers) that appeared red in the imagery. Other smaller coral specimens that appeared red could certainly have been missed and thus excluded from the count. Another situation that could lead to different determinations of percent cover is illustrated by the colonies of *P. porites*, recognizable as clusters of small bright targets (Figs. 6, 7B). The appearance results from the finger-like nature of the *Porites* colony with macroalgae growing in and around it. From the vantage point of FILLS, the colony occupies less area than would be assigned to the same feature by an interpreter of photographic imagery, who could exercise reasonable judgment and select the outer border of the entire colony as the boundary for determining projected surface area.

The FILLS sensor looks down on the reef surface from above, at angles ranging from vertical to  $\sim 35^\circ$ . With this perspective, it shares the same viewing limitations as video transect and other fly-over visualization techniques. Features can be hidden from view by other features that grow above them, and growth on vertical surfaces can be missed. Also, FILLS is limited to two-dimensional imaging of projected areas of features and does not capture their full three-dimensional structure.

Processing of the raw FILLS data must take into account attenuation of the fluoresced light in its passage from the subject on the seafloor to the sensor in the water column above. Water column attenuation begins to increase rapidly at wavelengths within the bandwidth of the 580-nm channel and is especially significant for the 685-nm channel (Smith and Baker 1981). The farther an imaged point is from the

centerline of the sensor, the more the light is attenuated. A systematic image processing routine works best on a uniform data set, so the imagery data must be corrected for the range to the image point. For a low-relief surface such as the Crosby’s Hump site, this requires that a slant range correction be applied, but the challenge is greater for a highly three-dimensional site such as the coral head at North Perry Reef. For the current work, phenomenologically based corrections were applied because detailed range information was not available. Efforts are being made to incorporate a bathymetric sonar with the FILLS sensor so that the ranges to pixels can be measured, allowing appropriate physically based corrections to be applied to the data. The increase in “black” pixels on the right edge of the Crosby’s Hump imagery, as shown in the steep upswing in Fig. 4F, could be due either to an insufficient correction for the slant range effect or to the onset of vignetting in that data set.

Although it is desirable to normalize signals throughout an image as much as possible by correcting for path length and spectral attenuation, it is also worthwhile to seek classification approaches that are somewhat insensitive to variations in absolute signal level and to imperfections in data postprocessing. Fluorescence imaging may have an advantage over multi- or hyperspectral imaging of reflected light in this regard because the range of possible responses is more constrained. The introductory section of this manuscript included an overview of the sources of fluorescence on the seafloor. There is certainly a variety of such responses, but they are limited enough that it may be possible to exploit classification metrics such as the ratio between two wavelength responses, rather than absolute signal levels. Informed selection of the detection wavelengths may help to counter the effects of spectral variation in attenuation. As long as there is sufficient dynamic range in the receiver, we hope to be able to achieve a degree of leeway in the requirement for signal normalization that eases the requirements for the collection of ancillary data, making the goal of a practical fluorescence imaging system more feasible.

The FILLS system was operated exclusively at night to avoid the influence of reflected solar illumination. This greatly simplified our image classification task, but for practical reasons, it would be desirable to be able to conduct surveys in the daytime as well. More modeling and experimental work are required to determine acceptable levels of ambient light and to develop schemes for measuring the reflected light during a survey, such as by taking periodic scans with the laser blocked. This could possibly enable the reflected component to be subtracted from the fluorescence plus reflectance signal.

The ability to assign a useful classification to every pixel in an image would be of great value for reef survey work. The very large number of sampling points,  $>3 \times 10^6$  for the Crosby’s Hump imagery, should provide reliable statistics. This level of data should also assist in the analysis of various sampling techniques. The coverage statistics derived from the simulated line transects exhibited a great deal of variability, strongly associated with the presence of discrete features such as barrel sponges or individual large coral colonies. If we had computed the statistics with points selected at 1-m intervals along the lines rather than using all 4,096

points, the variability would certainly have been greater. This demonstrates the sensitivity of the line transect method to small changes in the positioning of the transect line. One could use the fluorescence image to determine how many randomly placed transect lines, and with what sampling intervals, would be required to reproduce the full image statistics. Interestingly, the percent cover values computed from the grid pattern of 121-pixel boxes distributed over the image were close to those computed using all pixels in the image, despite amounting to only ~1% of the total pixels. This tells us something about the distribution of the benthic organisms at this particular location, but such a result might not be expected at other reef sites.

The data set could also be used to investigate spatial distribution characteristics of features of interest, such as the objects identified as cnidarians (Fig. 5). An application that would be of value would be computation of size-frequency distributions of corals as shown in Table 4, which might aid in assessing coral population dynamics (Bak and Meesters 1998). The Crosby's Hump data set was heavily weighted to very small objects, especially those consisting of only a single pixel. This may be more an artifact of the image collection and classification process than a true representation of the number of very small corals on the reef. Various effects can cause seafloor features to be accounted for incorrectly. For example, a gorgonian rising over a neighboring coral could result in the image of that coral being divided into two parts that would then be counted as two separate, smaller specimens. The *Palythoa* colonies illustrated in Fig. 2B account for numerous distinct objects in the FILLS imagery but would be counted as a single large colony in a diver or video survey. Isolated bright pixels could also be associated with system noise or with errors in the classification algorithms. Some could also be associated with other small fluorescing features that are not cnidarians, such as bristleworms. An interactive rather than fully automated approach to image classification could resolve some of these issues. It is also possible that the fluorescence imaging system does a better job than divers at finding very small specimens, and that many of the isolated pixels are legitimately associated with distinct features on the bottom. The FILLS data and our algorithms were not able to distinguish among coral species, and previous work indicates that expected size-frequency distributions may vary from one species to another (Bak and Meesters 1998).

There is still much to be learned about fluorescence and about the details of applying feature classifications to high-resolution multispectral fluorescence images of the reef before this imaging approach can be applied as a general tool. Observations indicate that in the case of coral fluorescence, for example, there can be variation in the fluorescence spectra and efficiencies within species both at a single site and from one site to another. Bleaching was not a factor at the FILLS study sites described here, but there may be significant fluorescence changes associated with that phenomenon (Hardy et al. 1992). Even at the current state of knowledge, though, repeated surveys of a single site could provide valuable data on changes in bottom cover type over time.

There is ample room for further development of the prototype FILLS sensor. New technology may enable the use

of other excitation wavelengths, and there is the potential to add more spectral detection bands for improved bottom classification. Other image classification algorithms could be developed that utilize the reflectance data as an adjunct to the fluorescence data, or that combine spatial with spectral analysis. New technology might also enable a reduction in the size and power requirements of the system, enabling construction of a version more suitable for widespread use. The initial trials described here suggest that laser fluorescence imaging has the potential to make valuable contributions to reef habitat mapping and assessment.

## References

- BAK, R. P. M., AND E. H. MEESTERS. 1998. Coral population structure: The hidden information of colony size-frequency distributions. *Mar. Ecol. Prog. Ser.* **162**: 301–306.
- BALLANTINE, D. L., J. N. NAVARRO, AND D. A. HENSLEY. 2001. Algal colonization of Caribbean scorpionfishes. *Bull. Mar. Sci.* **69**: 1089–1094.
- BOHNSACK, J. A. 1979. Photographic quantitative sampling of hard-bottom communities. *Bull. Mar. Sci.* **29**: 242–252.
- BOTO, K., AND P. ISDALE. 1985. Fluorescent bands in massive corals result from terrestrial fulvic acid inputs to nearshore zone. *Nature* **315**: 396–397.
- CATALA, R. 1959. Fluorescence effects from corals irradiated with ultra-violet rays. *Nature* **183**: 949.
- CROSBY, M. P., AND E. S. REESE. 1996. A manual for monitoring coral reefs with indicator species: Butterflyfishes as indicators of change on Indo-Pacific reefs. Office of Ocean and Coastal Resource Management, National Oceanic and Atmospheric Administration.
- DETHIER, M. N., E. S. GRAHAM, S. COHEN, AND L. M. TEAR. 1993. Visual versus random-point percent cover estimations: 'Objective' is not always better. *Mar. Ecol. Prog. Ser.* **96**: 93–100.
- DOVE, S. G., O. HOEGH-GULDBERG, AND S. RANGANATHAN. 2001. Major colour patterns of reef-building corals are due to a family of GFP-like proteins. *Coral Reefs* **19**: 197–204.
- HARDY, J. T., F. E. HOGE, J. K. YUNGEL, AND R. E. DODGE. 1992. Remote detection of coral 'bleaching' using pulsed-laser fluorescence spectroscopy. *Mar. Ecol. Prog. Ser.* **88**: 247–255.
- HOLDEN, H., AND E. LEDREW. 1999. Hyperspectral identification of coral reef features. *Int. J. Remote Sens.* **20**: 2545–2563.
- LABAS, Y. A., N. G. GURSKAYA, Y. G. YANUSHEVICH, A. F. FRADKOV, K. A. LUKYANOV, S. A. LUKYANOV, AND M. V. MATZ. 2002. Diversity and evolution of the green fluorescent protein family. *PNAS* **99**: 4256–4261.
- LARKUM, A. W. D., G. C. COX, R. G. HILLER, D. L. PARRY, AND T. P. DIBBAYAWAN. 1987. Filamentous cyanophytes containing phycourobilin and in symbiosis with sponges and an ascidian of coral reefs. *Mar. Biol.* **95**: 1–13.
- LEONARD, G. H., AND R. P. CLARK. 1993. Point quadrat versus video transect estimates of the cover of benthic red algae. *Mar. Ecol. Prog. Ser.* **101**: 203–208.
- LOGAN, A., K. HALCROW, AND T. TOMASCIK. 1990. UV excitation-fluorescence in polyp tissue of certain scleractinian corals from Barbados and Bermuda. *Bull. Mar. Sci.* **46**: 807–813.
- LOYA, Y. 1978. Plotless and transect methods, pp.197–218. *In* D. R. Stoddart and R. E. Johannes [eds.]. *Coral reefs: Research methods*. UNESCO.
- LUCZKOVICH, J. J., T. W. WAGNER, J. L. MICHALEK, AND R. W. STOFFLE. 1993. Discrimination of coral reefs, seagrass meadows, and sand bottom types from space: A Dominican Republic case study. *Photogramm. Eng. Remote Sens.* **59**: 385–389.

- MARAGOS, J. E., M. P. CROSBY, AND J. MCMANUS. 1996. Coral reefs and biodiversity: A critical and threatened relationship. *Oceanography* **9**: 83–99.
- MATTHEWS, B. J. H., A. C. JONES, N. K. THEODOROU, AND A. W. TUDHOPE. 1996. Excitation-emission-matrix spectroscopy applied to humic acid bands in coral reefs. *Mar. Chem.* **55**: 317–332.
- MATZ, M. V., A. F. FRADKOV, Y. A. LABAS, A. P. SAVITSKY, A. G. ZARAISKY, M. L. MARKELOV, AND S. A. LUKYANOV. 1999. Fluorescent proteins from nonbioluminescent Anthozoa species. *Nat. Biotechnol.* **17**: 969–973.
- MAZEL, C. H. 1995. Spectral measurements of fluorescence emission in Caribbean cnidarians. *Mar. Ecol. Prog. Ser.* **120**: 185–191.
- . 1997. Coral fluorescence characteristics: Excitation-emission spectra, fluorescence efficiencies, and contribution to apparent reflectance. *SPIE* **2963**: 240–245.
- , M. P. LESSER, M. Y. GORBUNOV, T. M. BARRY, J. H. FARRELL, K. D. WYMAN, AND P. G. FALKOWSKI. 2003. Green-fluorescent proteins in Caribbean corals. *Limnol. Oceanogr.* **48**: 402–411.
- MEESE, R. J., AND P. A. TOMICH. 1992. Dots on the rocks: A comparison of percent cover estimation methods. *J. Exp. Mar. Biol. Ecol.* **165**: 59–73.
- MORIN, J. G., AND J. W. HASTINGS. 1971. Biochemistry of the bioluminescence of colonial hydroids and other coelenterates. *J. Cell. Physiol.* **77**: 305–312.
- MUMBY, P. J., E. P. GREEN, C. D. CLARK, AND A. J. EDWARDS. 1998. Digital analysis of multispectral airborne imagery of coral reefs. *Coral Reefs* **17**: 59–69.
- NEVIS, A. J. 1999. Adaptive background equalization and image processing applications for laser line scan data. *SPIE* **3710**: 1260–1271.
- OHLHORST, S. L., W. D. LIDDELL, R. J. TAYLOR, AND J. M. TAYLOR. 1988. Evaluation of reef census techniques. *Proceedings of the 6th International Coral Reef Symposium* **2**: 319–324.
- PRASHER, D. C., V. K. ECKENRODE, W. W. WARD, F. G. PRENDERGAST, AND M. J. CORMIER. 1992. Primary structure of the *Aequorea victoria* green-fluorescent protein. *Gene* **111**: 229–233.
- RÜTZLER, K., D. L. SANTAVY, AND A. ANTONIUS. 1983. The black band disease of Atlantic reef corals. III. Distribution, ecology, and development. *PSZNI Mar. Ecol.* **4**: 329–358.
- SHEPPARD, C. R. C., K. MATHESON, J. C. BYTHELL, P. MURPHY, C. B. MYERS, AND B. BLAKE. 1995. Habitat mapping in the Caribbean for management and conservation: Use and assessment of aerial photography. *Aquat. Conserv. Mar. Freshw. Ecosyst.* **5**: 277–298.
- SIMON-BLECHER, N., Y. ACHITUV, AND Z. MALIK. 1996. Effect of epibionts on the microdistribution of chlorophyll in corals and its detection by fluorescence spectral imaging. *Mar. Biol.* **126**: 757–763.
- SMITH, R. C., AND K. S. BAKER. 1981. Optical properties of the clearest natural waters (200–800 nm). *Appl. Opt.* **20**: 177–184.
- STRAND, M. P. 1997. Underwater electro-optical system for mine identification. *Nav. Res. Rev.* **49**: 20–28.
- STRAND, M. P., B. W. COLES, A. J. NEVIS, AND R. REGAN. 1997. Laser line scan fluorescence and multispectral imaging of coral reef environments. *SPIE* **2963**: 790–795.
- TOPINKA, J. A., W. KORJEFF BELLOWES, AND C. S. YENTSCH. 1990. Characterization of marine macroalgae by fluorescence signatures. *Int. J. Remote Sens.* **11**: 2329–2335.
- TUCKER, M. E., AND V. P. WRIGHT. 1990. *Carbonate sedimentology*. Blackwell Science.
- WHORF, J. S., AND L. GRIFFING. 1992. A video recording and analysis system used to sample intertidal communities. *J. Exp. Mar. Biol. Ecol.* **160**: 1–12.
- WILKINSON, C. R., AND P. FAY. 1979. Nitrogen fixation in coral reef sponges with symbiotic cyanobacteria. *Nature* **279**: 527–529.
- WITMAN, J. D. 1985. Refuges, biological disturbance, and rocky subtidal community structure in New England. *Ecol. Monogr.* **55**: 421–445.

Received: 28 September 2001

Accepted: 18 April 2002

Amended: 13 May 2002